

Optical Properties and Thermal Stability of a Cubic Sulfate $\text{Rb}_2\text{Ca}_2(\text{SO}_4)_3$ ^①

ZHONG Xiao-Yu WU En-Qiang YANG Sheng-Dong
WANG Hao-Hang LIN Xiao-Xin SHEN Yao-Guo^②

(College of Physics & Electronic Information Engineering, Minjiang University, Fuzhou 350108, China)

ABSTRACT In this paper, a non-centrosymmetric compound of $\text{Rb}_2\text{Ca}_2(\text{SO}_4)_3$ has been synthesized by a high temperature solid-state reaction and high temperature melting method. Single-crystal X-ray diffraction analysis shows that $\text{Rb}_2\text{Ca}_2(\text{SO}_4)_3$ crystallizes in the cubic space group of $P2_13$, and its cell parameters are $a = b = c = 10.5569(6)$ Å, $Z = 4$ and $V = 1176.55(12)$ Å³, respectively. In the crystal structure, SO_4 tetrahedra and CaO_6 octahedra are connected with each other by a corner-sharing mode to construct the three-dimensional framework of $\text{Rb}_2\text{Ca}_2(\text{SO}_4)_3$. Optical measurements show that the title compound has a short ultraviolet absorption edge and a moderate second-harmonic generation response. The optical origin is illustrated by the electron band structure calculation. In addition, thermal stability is also studied by virtue of differential thermal/thermogravimetric analysis and powder XRD technique.

Keywords: crystal structure, nonlinear optics, solid-state reaction, sulfate;

DOI: 10.14102/j.cnki.0254-5861.2011-3047

1 INTRODUCTION

Nonlinear optical (NLO) crystals are important photoelectrical information functional materials in information optics, photolithography, medical treatment and other fields. A commercially available short-wave NLO material needs to meet some conditions, such as a non-centrosymmetric structure, short cut-off edge, large second-harmonic generation (SHG) response, good thermal stability, and crystal easy to grow. In addition, the use of toxic elements should be avoided in the process of crystal preparation^[1]. According to the inorganic crystal structure database, most reported compounds have a central symmetry structure, and the probability of obtaining non-centrosymmetric compounds is relatively low^[2]. Consequently, it is still a challenge to design and construct a new NLO material which can work in the short-wave spectral region^[3].

In the past few decades, the search for short-wave NLO materials has been typically limited to borates, because NLO-active triangle BO_3 groups in borates have comprehensive performance^[4]. Many excellent NLO borates have been synthesized like $\text{KBe}_2\text{BO}_3\text{F}_2$ ^[5], $\text{Li}_6\text{Zn}_3(\text{BO}_3)_4$ ^[6] and $\text{Li}_4\text{Sr}(\text{BO}_3)_2$ ^[7]. Due the short ultraviolet cut-off edge of PO_4

groups, phosphates have also received the attention of researchers, and some short-wave NLO phosphates with good performance are reported recently, such as $\text{Ba}_3\text{P}_3\text{O}_{10}\text{X}$ ($\text{X} = \text{Cl}, \text{Br}$)^[8], LiCs_2PO_4 ^[9], LiRb_2PO_4 ^[10] and $\text{Na}_3\text{Cd}_3\text{B}(\text{PO}_4)_4$ ^[11]. Because SO_4 groups have the same tetrahedral configuration as PO_4 groups, sulfates are expected to have similar NLO properties as phosphates. Introducing ammonium ions and alkali metal elements into sulfates, Luo group reported two NLO sulfates of $\text{NH}_4\text{NaLi}(\text{SO}_4)_2$ and $(\text{NH}_4)_2\text{Na}_3\text{Li}_9(\text{SO}_4)_7$ in 2019^[8]. Both compounds can be used in deep ultraviolet region, and their SHG responses reach 1.1 and 0.5 times that of KH_2PO_4 , respectively, indicating that sulfates are expected to be good candidates for deep ultraviolet NLO materials.

After investigation and research, it is reported that alkali metal and alkali-earth metal elements can improve the thermal stability of compounds^[3]. Therefore, we screened the alkali metal and alkali-earth metal sulfate systems in the inorganic crystal structure database and selected $\text{Rb}_2\text{Ca}_2(\text{SO}_4)_3$ ^[12] as the subject of study. In this context, the thermal stability, SHG effect and diffuse reflectance spectrum of $\text{Rb}_2\text{Ca}_2(\text{SO}_4)_3$ will be studied. In addition, its optical origin is analyzed by virtue of structure and theoretical calculation.

Received 23 November 2020; accepted 4 January 2021 (CCDC 2041017)

① This research was supported by the Doctoral Fund (MJY19014), Natural Science Foundation of Fujian Province (2019J01762), and President's Fund (103952020020)

② Corresponding author. Shen Yao-Guo, male, associate professor, doctor's degree. E-mail: shenyg@mju.edu.cn

Zhong Xiao-Yu and Wu En-Qiang contributed equally to this work

2 EXPERIMENTAL

2.1 Materials and methods

Rb_2SO_4 (99.0%) and CaSO_4 (99.0%) were purchased from Aladdin and used without further purification. Differential thermal/Thermogravimetric analysis (DTA/TGA) was tested on a NETZSCH STA 449F3 simultaneous analyzer with bubbling nitrogen as the purge gas. The powder X-ray diffraction (XRD) data were collected on a Rigaku MiniFlex II diffractometer ($\text{CuK}\alpha$ radiation). The sampling range, interval and scanning rate are $2\theta = 10^\circ \sim 70^\circ$, 0.02° and $0.4^\circ \text{min}^{-1}$, respectively. UV/Vis/NIR diffuse reflectance spectrum was collected using a PerkinElmer lambda-950 UV/Vis/NIR dispersive photometer at ambient temperature.

2.2 Synthesis of $\text{Rb}_2\text{Ca}_2(\text{SO}_4)_3$

Pure polycrystalline $\text{Rb}_2\text{Ca}_2(\text{SO}_4)_3$ was synthesized by a convenient high temperature solid-state reaction^[12]. First, the above-mentioned chemical reagents were weighed at the molar ratio of $\text{Rb}_2\text{SO}_4/\text{CaSO}_4 = 1/2$, and then ground evenly with an agate mortar. Secondly, the mixture after grinding was placed in a platinum crucible followed by sintering at 973 K for 5000 min. In the calcining process, the mixture was ground twice. The purity of the prepared product was monitored by powder XRD analysis.

The technique of spontaneous crystallization is used to prepare $\text{Rb}_2\text{Ca}_2(\text{SO}_4)_3$ single crystal. Firstly, Rb_2SO_4 and CaSO_4 were mixed in the molar ratio of 1/3, and roasted at 1073 K in the electric stove for 2000 min. The nominal polycrystalline $\text{Rb}_2\text{Ca}_3(\text{SO}_4)_4$ was obtained after cooling to room temperature. Secondly, the target compound of $\text{Rb}_2\text{Ca}_2(\text{SO}_4)_3$ was synthesized by melting the mixture of $\text{Rb}_2\text{Ca}_3(\text{SO}_4)_4$ and Rb_2SO_4 in the molar ratio of $\text{Rb}_2\text{SO}_4/\text{Rb}_2\text{Ca}_2(\text{SO}_4)_3 = 1/3$. Transparent $\text{Rb}_2\text{Ca}_2(\text{SO}_4)_3$ single crystal can be selected to determine the single-crystal structure.

2.3 X-ray structure determination

A colorless block crystal was selected and stuck on a glass fiber for data collection performed on a Bruker D8 diffractometer at 200(2) K using graphite-monochromatic $\text{MoK}\alpha$ radiation ($\lambda = 0.71073 \text{ \AA}$). Data simplification and absorption correction were performed on APEX3 program. In SHELXS program, the structure was solved by direct methods and then refined by full-matrix least-squares program SHELXL^[13] including anisotropic displacement parameters. Finally, the rationality of the structure was tested by PLATON^[14]. Crystal data for $\text{Rb}_2\text{Ca}_2(\text{SO}_4)_3$ ($M_r = 539.28$

g/mol): cubic system, space group $P2_13$, $a = 10.5569(6)$, $b = 10.5569(6)$, $c = 10.5569(6) \text{ \AA}$, $V = 1176.55(12) \text{ \AA}^3$, $Z = 4$, $T = 200(2) \text{ K}$, $\mu(\text{MoK}\alpha) = 9.780 \text{ mm}^{-1}$, $D_c = 3.044 \text{ g/cm}^3$, 7615 reflections measured ($3.34^\circ \leq \theta \leq 27.41^\circ$) and 904 unique ($R_{\text{int}} = 0.0399$, $R_{\text{sigma}} = 0.0379$) which were used in all calculations. The final $R = 0.0174$ ($I > 2\sigma(I)$) and $wR = 0.0391$ (all data).

2.4 Second-harmonic generation measurement

Using the innovative Kurtz and Perry method^[15], the SHG signal of $\text{Rb}_2\text{Ca}_2(\text{SO}_4)_3$ was recorded under the 1064 nm beam generated by the Q-switched Nd:YAG laser. The polycrystalline material was placed between the glass sheets and pressed into a circular box with a diameter of 8 mm. The samples were irradiated with 1064 nm laser and the output SHG signal was recorded by photomultiplier tube. In the same environment and operation steps, KH_2PO_4 was also tested as a comparison.

2.5 Methods of calculation

The density of states and electronic energy band were calculated by using the CASTEP program of density functional theory in the software package of material studio^[16, 17]. The function of generalized gradient approximation (GGA) model proposed by Perdew Burke emzerhoff (PBE)^[18, 19] was selected to record the performance of the exchange correlation. Most atoms use soft pseudopotential^[20]. The energy cutoff momentum was set to 300 eV, and $2 \times 2 \times 2$ k -point grid in Brillouin region was selected for the title compound.

3 RESULTS AND DISCUSSION

3.1 Synthesis and characterization

Polycrystalline $\text{Rb}_2\text{Ca}_2(\text{SO}_4)_3$ was synthesized by a convenient high temperature solid state reaction. Its purity was confirmed by powder XRD analysis in the range of $2\theta = 10^\circ \sim 70^\circ$ (Fig. 1). The experimental curve agrees well with the calculated one, which verifies the pure of polycrystalline $\text{Rb}_2\text{Ca}_2(\text{SO}_4)_3$. In the heating run of DTA curve (Fig. 2), there is one endothermic peak in the temperature range of 1200~1300 K. After DTA experiment, the residue clumps together. Moreover, the TGA curve is almost a straight line, which confirms that most of the mass is preserved in the whole experiment. The DTA and TGA suggest that $\text{Rb}_2\text{Ca}_2(\text{SO}_4)_3$ did not break into other products. To confirm this speculation, $\text{Rb}_2\text{Ca}_2(\text{SO}_4)_3$ polycrystalline were melted at 1323 K in a muffle furnace for 11 hours and then cool

slowly to outdoor temperature. The material was ground for powder XRD analysis and its XRD curve fits perfectly with

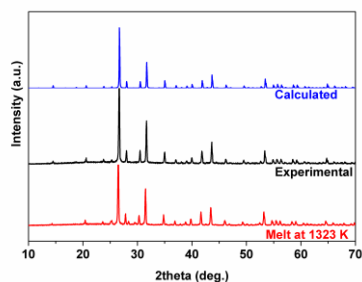


Fig. 1. Calculated, experimental and sintered XRD patterns for $\text{Rb}_2\text{Ca}_2(\text{SO}_4)_3$

the experimental one. All these results bear out the high thermal stability of the title compound.

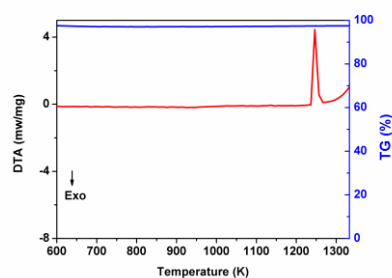


Fig. 2. DTA/TGA curve of $\text{Rb}_2\text{Ca}_2(\text{SO}_4)_3$

3.2 X-ray crystal structure

In the single crystal structure of $\text{Rb}_2\text{Ca}_2(\text{SO}_4)_3$, the crystallographic positions of Rb, Ca, S, and O are 2, 2, 1 and 4, respectively. The 3D framework is composed of SO_4 tetrahedra and CaO_6 octahedra which are connected with each other in a corner-sharing mode (Fig. 3). Rb^+ cations fill in the gap of the 3D framework to maintain the electrical neutrality of the compound. The bond distances of S–O,

Ca–O and Rb–O lie in the ranges of 1.453(2)~1.462(2) Å, 2.298(2) ~ 2.330(2) Å and 3.017(2) ~ 3.455(3) Å, respectively. The bond angles of O–S–O vary from 108.35(15)° to 110.69(15)°, indicating the SO_4 functional group is basically a regular tetrahedron. These data are generally reasonable according to the reported sulfates^[8, 12]. Detailed bond parameters are listed in Table 1.

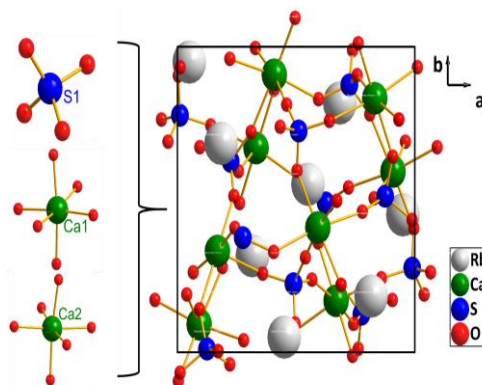


Fig. 3. A ball-and-stick representation of $\text{Rb}_2\text{Ca}_2(\text{SO}_4)_3$. (a) SO_4 tetrahedron and CaO_6 octahedra; (b) 3D framework

Table 1. Selected Bond Lengths (Å) and Bond Angles (°)

Bond	Dist.	Bond	Dist.	Bond	Dist.
Rb(1)–O(1)c	3.235(3)	Rb(2)–O(4)f	3.324(3)	S(1)–O(1)	1.462(2)
Rb(1)–O(3)a	3.022(3)	Ca(1)–O(3)	2.303(2)	S(1)–O(2)	1.459(2)
Rb(1)–O(4)	3.455(3)	Ca(1)–O(4)b	2.302(2)	S(1)–O(3)	1.453(2)
Rb(2)–O(1)f	3.107(2)	Ca(2)–O(1)	2.298(2)	S(1)–O(4)	1.460(2)
Rb(2)–O(2)e	3.017(2)	Ca(2)–O(2)d	2.330(2)		
Angle	(°)	Angle	(°)	Angle	(°)
O(1)–Ca(2)–O(1)g	85.87(9)	O(1)g–Ca(2)–O(2)d	88.40(8)	O(4)h–Ca(1)–O(3)e	90.81(9)
O(1)–Ca(2)–O(2)i	88.41(8)	O(2)d–Ca(2)–O(2)i	96.49(9)	O(4)c–Ca(1)–O(3)e	80.72(10)
O(1)g–Ca(2)–O(2)i	172.38(9)	O(3)e–Ca(1)–O(3)	97.24(9)	O(4)b–Ca(1)–O(3)e	171.89(9)
O(1)–Ca(2)–O(2)d	88.72(9)	O(4)c–Ca(1)–O(4)b	91.44(9)	O(3)–S(1)–O(2)	110.60(14)
O(3)–S(1)–O(4)	108.35(15)	O(2)–S(1)–O(4)	109.95(16)	O(3)–S(1)–O(1)	110.69(15)

Symmetry transformation: a: $z-1/2, -x+3/2, -y+2$; b: $-y+3/2, -z+2, x+1/2$; c: $x+1/2, -y+3/2, -z+2$; d: y, z, x ; e: z, x, y ;

f: $-x+1, y-1/2, -z+3/2$; g: $y-1/2, -z+3/2, -x+1$; h: $-z+2, x+1/2, -y+3/2$; i: $-x+1, y+1/2, -z+3/2$

The valences for the cations in $\text{Rb}_2\text{Ca}_2(\text{SO}_4)_3$, which calculated by the bond-valence-sum method^[21, 22], are consistent with their normal valence states (Rb, 1+; Ca, 2+; S, 6+).

3.3 UV/Vis/NIR diffuse reflectance spectroscopy

The diffuse reflectance spectrum of the title compound was measured by a UV/Vis/NIR spectrophotometer in ambient temperature. The incident light wavelength was set in the range of 200~800 nm. Firstly, BaSO_4 powder was tested, and its reflectivity was set as the reference; then, a

few samples were laid on the surface of BaSO_4 powder and tested under the same conditions. The result is shown in Fig. 4. In the whole visible light region, the reflectance is as high as 80%. When the incident light wavelength is as low as 200 nm, the reflectivity is still above 80%, indicating that the UV cut-off edge of $\text{Rb}_2\text{Ca}_2(\text{SO}_4)_3$ is lower than 200 nm. The fine UV transparency can also be visually observed from the transformed absorption curve in the energy range of 0~6.2 eV.

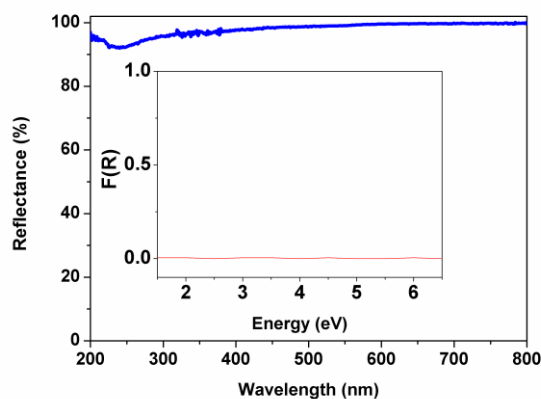


Fig. 4. UV/Vis/NIR diffuse-reflectance spectrum of $\text{Rb}_2\text{Ca}_2(\text{SO}_4)_3$. The inset represents the absorption curve

3.4 Nonlinear optical properties

The main requirement of NLO response is that the inorganic compound should crystallize in a non-centrosymmetric structure. Therefore, it is an effective way to test the structure using the SHG measurement. The SHG measurement of $\text{Rb}_2\text{Ca}_2(\text{SO}_4)_3$ powder was tested at ambient

temperature. Commercial KH_2PO_4 samples were used for comparison. In the particle range of 0~63 μm , the magnitude of SHG signal is about $0.3 \times \text{KH}_2\text{PO}_4$ (Fig. 5), which proves that $\text{Rb}_2\text{Ca}_2(\text{SO}_4)_3$ belongs to a non-centrosymmetric structure.

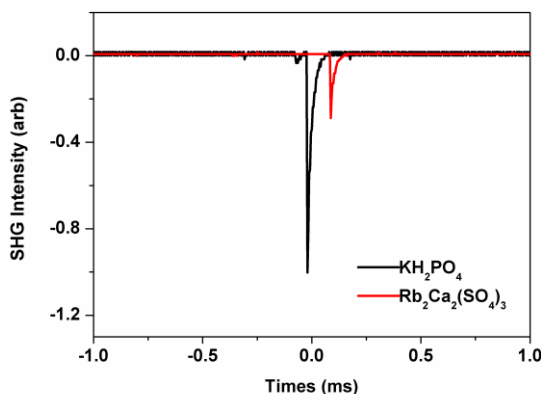


Fig. 5. SHG signal of $\text{Rb}_2\text{Ca}_2(\text{SO}_4)_3$ and KH_2PO_4 under a 1064 nm laser radiation

3.5 Electronic structure

In order to reveal the structure property relationship of $\text{Rb}_2\text{Ca}_2(\text{SO}_4)_3$, theoretical calculation was carried out. Fig. 6a

shows band structure diagram in which $\text{Rb}_2\text{Ca}_2(\text{SO}_4)_3$ has a theoretical energy gap of 5.63 eV, which is basically consistent with the diffuse reflectance spectrum. Fig. 6b

shows the density of states (DOS) and partial DOS. It is well known that the electronic energy level transition near Fermi energy level has an important influence on the optical properties of a compound. At the top of the valence band ranging from -10 to 0 eV, the DOS are predominately occupied by O $2p$ and S $3p$ orbitals. Near the band gap

ranging from 5 to 10 eV, the conduction band is mainly originated from Rb $5s$ and S $3s$. Notably, the Ca^{2+} cations have negligible contribution to DOS^[23]. In other words, RbO_n and SO_4 groups have important contributions to DOS near the forbidden zone. As a result, they play a decisive role in optical properties.

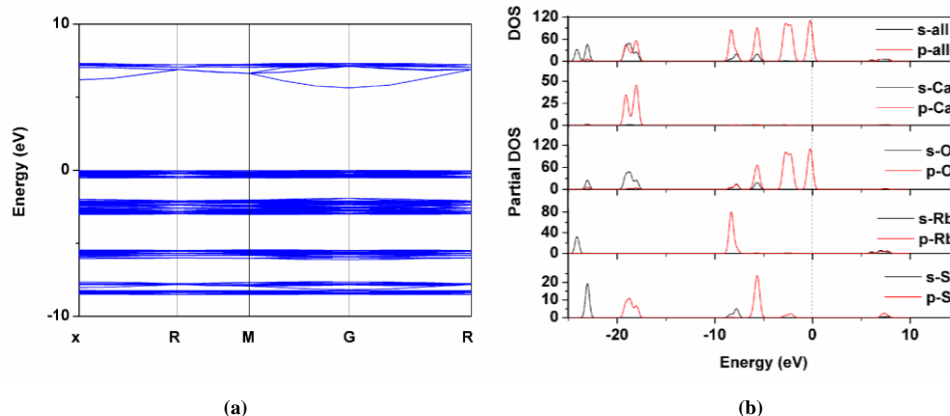


Fig. 6. (a) Electronic band structure, (b) DOS and partial DOS plots

4 CONCLUSION

In summary, pure polycrystalline $\text{Rb}_2\text{Ca}_2(\text{SO}_4)_3$ was synthesized by a high temperature solid-state reaction. Single-crystal diffraction measurement results indicate $\text{Rb}_2\text{Ca}_2(\text{SO}_4)_3$ belongs to $P2_13$ space group, and it features a 3D framework consisting of SO_4 tetrahedra and CaO_6 octahedra. The Rb ions fill the holes in the framework. The crystal is stable below 1200 K. The UV cut-off edge of

$\text{Rb}_2\text{Ca}_2(\text{SO}_4)_3$ is lower than 200 nm. In addition, the SHG response of this crystal is about 0.3 times that of KH_2PO_4 . The theoretical calculation about electron band structure and density of states indicates that RbO_n and SO_4 groups have the most important contribution to the optical properties. The above results show that alkali metal and alkaline-earth metal sulfates may have potential applications as short-wave NLO materials.

REFERENCES

- (1) Li, Y. Q.; Luo, J. H.; Ji, X. H.; Zhao, S. G. A short-wave UV nonlinear optical sulfate of high thermal stability. *Chin. J. Struct. Chem.* **2020**, *39*, 485–492.
- (2) Huang, L.; Zou, G. H. Recent progresses of UV nonlinear optical materials. *Chin. J. Struct. Chem.* **2020**, *39*, 1571–1577.
- (3) Shen, Y. G.; Xue, X. L.; Tu, W. Y.; Liu, Z. Q.; Yan, R. W.; Zhang, H.; Jia, J. R. Synthesis, crystal structure, and characterization of a noncentrosymmetric sulfate $\text{Cs}_2\text{Ca}_2(\text{SO}_4)_3$. *Eur. J. Inorg. Chem.* **2020**, 2020, 854–858.
- (4) Chen, J.; Ali, K. M.; Xiao, C. X.; Yan, Y. X.; Dai, Y.; Chen, L. Recent advances in nonlinear optical phosphate materials. *Chin. J. Struct. Chem.* **2017**, *36*, 1837–1858.
- (5) Zhang, X.; Wang, Z. M.; Wang, G. L.; Zhu, Y.; Xu, Z. Y.; Chen, C. T. Widely tunable and high-average-power fourth-harmonic generation of a Ti:sapphire laser with a $\text{KBe}_2\text{BO}_3\text{F}_2$ prism-coupled device. *Opt. Lett.* **2009**, *34*, 1342–1344.
- (6) Chen, Y. N.; An, D. H.; Zhang, M.; Hu, C.; Mutailipu, M.; Yang, Z. H.; Lu, X. Q.; Pan, S. L. $\text{Li}_6\text{Zn}_3(\text{BO}_3)_4$: a new zincoborate featuring vertex-, edge- and face-sharing LiO_4 tetrahedra and exhibiting reversible phase transitions. *Inorg. Chem. Front.* **2017**, *4*, 1100–1107.
- (7) Zhao, S. G.; Gong, P. F.; Bai, L.; Xu, X.; Zhang, S. Q.; Sun, Z. H.; Lin, Z. S.; Hong, M. C.; Chen, C. T.; Luo, J. H. Beryllium-free $\text{Li}_4\text{Sr}(\text{BO}_3)_2$ for deep-ultraviolet nonlinear optical applications. *Nat. Commun.* **2014**, *5*, 4019.
- (8) Li, Y.; Liang, F.; Zhao, S.; Li, L.; Wu, Z.; Ding, Q.; Liu, S.; Lin, Z.; Hong, M.; Luo, J. Two non- π -conjugated deep-UV nonlinear optical sulfates. *J. Am. Chem. Soc.* **2019**, *141*, 3833–3837.

- (9) Li, L.; Wang, Y.; Lei, B. H.; Han, S. J.; Yang, Z. H.; Poepelmeier, K. R.; Pan, S. L. A new deep-ultraviolet transparent orthophosphate LiCs_2PO_4 with large second harmonic generation response. *J. Am. Chem. Soc.* **2016**, 138, 9101–9104.
- (10) Li, L.; Wang, Y.; Lei, B. H.; Han, S. J.; Yang, Z. H.; Li, H. Y.; Pan, S. L. LiRb_2PO_4 : a new deep-ultraviolet nonlinear optical phosphate with a large SHG response. *J. Mater. Chem. C* **2017**, 5, 269–274.
- (11) Shi, Y.; Pan, S.; Dong, X.; Wang, Y.; Zhang, M.; Zhang, F.; Zhou, Z. $\text{Na}_3\text{Cd}_3\text{B}(\text{PO}_4)_4$: a new noncentrosymmetric borophosphate with zero-dimensional anion units. *Inorg. Chem.* **2012**, 51, 10870–10875.
- (12) Boujelben, M.; Toumi, M.; Mhiri, T. Langbeinite-type $\text{Rb}_2\text{Ca}_2(\text{SO}_4)_3$. *Acta Crystallogr., Sect. E: Cryst. Commun.* **2007**, 63, I157–U162.
- (13) Sheldrick, G. M. A short history of SHELX. *Acta Crystallogr., Sect. A: Found. Crystallogr.* **2008**, 64, 112–122.
- (14) Spek, A. L. Single-crystal structure validation with the program PLATON. *J. Appl. Crystallogr.* **2003**, 36, 7–13.
- (15) Kurtz, S. K.; Perry, T. T. A powder technique for the evaluation of nonlinear optical materials. *J. Appl. Phys.* **1968**, 39, 3798–3813.
- (16) Payne, M. C.; Teter, M. P.; Allan, D. C.; Arias, T. A.; Joannopoulos, J. D. Iterative minimization techniques for *ab initio* total-energy calculations: molecular dynamics and conjugate gradients. *Rev. Mod. Phys.* **1992**, 64, 1045–1097.
- (17) Clark, S. J.; Segall, M. D.; Pickard, C. J.; Hasnip, P. J.; Probert, M. J.; Refson, K.; Payne, M. C. First principles methods using CASTEP. *Z. Kristallogr. - Cryst. Mater.* **2005**, 220, 567–570.
- (18) Ceperley, D. M.; Alder, B. J. Ground-state of the electron-gas by a stochastic method. *Phys. Rev. Lett.* **1980**, 45, 566–569.
- (19) Perdew, J. P.; Zunger, A. Self-interaction correction to density-functional approximations for many-electron systems. *Phys. Rev. B: Condens. Matter Mater. Phys.* **1981**, 23, 5048–5079.
- (20) Rappe, A. M.; Rabe, K. M.; Kaxiras, E.; Joannopoulos, J. D. Optimized pseudopotentials. *Phys. Rev. B: Condens. Matter Mater. Phys.* **1990**, 41, 1227–1230.
- (21) Brown, I. D.; Altermatt, D. Bond-valence parameters obtained from a systematic analysis of the inorganic crystal-structure database. *Acta Crystallogr., Sect. B: Struct. Sci.* **1985**, 41, 244–247.
- (22) Brese, N. E.; O'Keeffe, M. Bond-valence parameters for solids. *Acta Crystallogr., Sect. B: Struct. Sci.* **1991**, 47, 192–197.
- (23) Lee, M. H.; Yang, C. H.; Jan, J. H. Band-resolved analysis of nonlinear optical properties of crystalline and molecular materials. *Phys. Rev. B* **2004**, 70, 235110